Surface & Coatings Technology 231 (2013) 247–252

Contents lists available at ScienceDirect

Surface & Coatings Technology

journal homepage: www.elsevier.com/locate/surfcoat

The effect of Cr/Zr chemical composition ratios on the mechanical properties of CrN/ZrN multilayered coatings deposited by cathodic arc deposition system

Siao-Fan Chen [a], Yu-Chu Kuo [a], Chaur-Jeng Wang [a], Sung-Hsiu Huang [b,c], Jyh-Wei Lee [d,e,*], Yu-Chen Chan [f], Hsien-Wei Chen [f], Jenq-Gong Duh [f], Tsung-Eong Hsieh [c]

[a] Dept. of Mechanical Engineering, National Taiwan University of Science and Technology, Taiwan
[b] Gigastorage Corp., Taiwan
[c] Department of Materials Science and Engineering, National Chiao Tung University, Taiwan
[d] Dept. of Materials Engineering, Ming Chi University of Technology, Taiwan
[e] Center for Thin Films Technologies and Applications, Ming Chi University of Technology, Taiwan
[f] Dept. of Materials Science and Engineering, National Tsing Hua University, Taiwan

ARTICLE INFO

Available online 8 March 2012

Keywords:
CrN/ZrN multilayered thin film
Cathode arc deposition system
Cr/Zr atomic ratio
Adhesion property

ABSTRACT

CrN/ZrN multilayer coatings with various Cr/Zr chemical compositions ratio were fabricated by a cathode arc deposition system. The Cr/Zr atomic ratios of the CrN/ZrN multilayer coatings were controlled, ranging from 1 to 2.5. The chemical composition of CrN/ZrN multilayer thin films was determined by a field emission electron probe microanalyzer (FE-EPMA). The phase composition of multilayer coatings was analyzed by a glancing angle X-ray diffractometer. Microstructures of the thin films were examined by field emission scanning electron microscopy (FE-SEM). Nanoindentation, the Daimler−Benz Rockwell-C (HRC-DB) adhesion, microhardness, pin-on-disc wear tests and scratch tests were used to evaluate the hardness, adhesion, toughness and tribological properties of the thin films, respectively. It was found that the hardness and tribological properties were strongly influenced by the Cr/Zr chemical composition ratios of the CrN/ZrN multilayer coatings. Optimal mechanical properties and the maximum hardness of 28 GPa were achieved for the coating when the Cr/Zr atomic ratio was 2.1.

1. Introduction

The cathodic arc evaporation (CAE) process is a promising, successful deposition method to fabricate multilayered hard coatings in tooling and forming industries, such as on saw blades, due to good wear and corrosion resistance [1–3]. Among the transition metal nitride based multilayered coating systems, only limited reports are available on CrN/ZrN multilayered coatings with different bilayer period thicknesses, Λ [4,5]. According to the research work by Zhang et al. [6,7], the tribological properties for direct current (DC) magnetron sputtered CrN/ZrN multilayered coatings were improved when the bilayer period thicknesses was 1.5 nm, whereas higher resistance to plastic deformation was revealed by CrSiN/ZrN multilayered coatings. On the other hand, the corrosion resistance of radio frequency (RF) magnetron sputtered CrN/ZrN multilayered coatings increased with increasing Λ values [8]. The CAE fabricated CrN/ZrN multilayered coating was applied to interior surfaces of Al bipolar plates when fabricating a polymer electrolyte membrane fuel cell [9]. On the other hand, the tribocorrosion behavior of CrN/ZrCN multilayered system deposited by CAE has been discussed [10]. In a previous work [11], the effects of the Λ on the mechanical properties of CAE deposited CrN/ZrN multilayered coatings were studied. The maximum hardness, 25.2 GPa, was achieved at Λ = 16 nm. However, for the CrN/ZrN multilayered coatings with the same bilayer period thickness, the influences of chemical composition ratio of Cr/Zr, or thickness ratio of CrN to ZrN layer, ℓ_{CrN}/ℓ_{ZrN} on the mechanical properties of coatings have not been reported in the literature. Meanwhile, the various thickness ratios, $\ell_{CrSiN}/\ell_{TiAlN}$, appeared to influence the mechanical properties of TiAlN/CrSiN multilayered coatings in a previous study [12].

In this work, the CAE process was employed to fabricate CrN/ZrN multilayered coatings with fixed Λ = 16 nm on titanium carbide (TiC) and Si substrates. The average hardness of TiC substrate is 26 GPa, which is used for the thin film adhesion evaluation. The Si substrates were adopted for the examination of cross-sectional morphology and thickness analysis for each coating. The effect of chemical composition ratio of Cr/Zr, or thickness ratio of CrN to ZrN layer,ℓ_{CrN}/ℓ_{ZrN}, on the microstructure, hardness, toughness and tribological properties is discussed. The motivation of this work is to propose a suitable chemical composition ratio of Cr/Zr, or thickness ratio of CrN to ZrN layer for CrN/ZrN multilayer thin films to

* Corresponding author at: Dept. of Materials Engineering, Ming Chi University of Technology, Taiwan. Tel.: +886 2 29089899x4437; fax: +886 2 29084091.

0257-8972/$ – see front matter © 2012 Elsevier B.V. All rights reserved.
doi:10.1016/j.surfcoat.2012.03.002

achieve high hardness, good adhesion and tribological performance, so as to be useful as a wear resistant coating in the tooling industry.

2. Experimental procedure

Four CrN/ZrN multilayered thin films with fixed Λ = 16 nm and different Cr/Zr atomic ratios, or different ℓ_{CrN}/ℓ_{ZrN} ratios were deposited on P-type (100) silicon wafers and TiC substrates by a cathodic arc evaporation system. Monolayer CrN and ZrN coatings were also fabricated for comparison. Cr and Zr targets with 99.99 wt.% purity, 101.6 mm in diameter were used. The Zr and Cr targets were in opposite positions and the substrates were mounted on two sides of a rotating barrel between the two targets. Multilayered coatings were deposited by alternately rotating the substrates between the plasma of Cr and Zr targets. The target current ratios of Cr and Zr were adjusted from 1.5 to 0.6 to achieve various Cr/Zr atomic ratios, i.e., different thickness ratios of CrN to ZrN layer (ℓ_{CrN}/ℓ_{ZrN}). The same bilayer period Λ was achieved by controlling the substrate holder rotation speed in the plasma stream from the Cr or Zr target. The thickness values of CrN/ZrN multilayer coatings were around 565 to 577 nm. The typical deposition conditions for each coating are listed in Table 1.

The chemical composition of the coatings was determined by a field emission electron probe microanalyzer (FE-EPMA, JXA-8500F, JEOL, Japan). Glancing angle X-ray diffractometer (XRD-6000, Shimadzu, Japan) with an incidence angle of 2° was utilized to study the crystal structure of each coating. The precise lattice parameter, a_0, of each film was calculated according to the following equation [13]:

$$a = a_0 + K \times \frac{\cos^2\theta}{\sin\theta} \tag{1}$$

where a is lattice contact, K is constant, ranging from 0.0057 to 0.0019 for different films, and θ is the diffraction angle. The low-angle X-ray reflectivity (XRR) technique was utilized to study the Λ of each multilayer coating. The surface roughness of each thin film deposited on the silicon substrate was analyzed by atomic force microscopy (DI-3100, Bruker, USA) with a scan area of 5 × 5 μm. The cross-sectional morphologies of coatings on Si substrates were observed by field emission scanning electron microscopy (FE-SEM, JSM-6701F, JEOL, Japan) and transmission electron microscopy (TEM, JSM-2100, JEOL, Japan). The TEM specimen was prepared using the dual beam Focused Ion Beam (FIB, FEI Quanta 3D FEG, USA). The nanohardness and elastic modulus of thin films on Si substrates were measured by means of a nanoindenter (TI-900, TriboIndenter, Hysitron, USA) using a Berkovich 142.3° diamond probe at a maximum applied load of 5 mN. Ten indentations were made on the surface for each coating. The maximum indentation depth was limited to around 50–60 nm, which was around one-tenth of the film thickness. The loading and unloading rates of the nanoindentation were all 1000 μN/s. The holding time was 5 s. The hardness and elastic modulus of each indent were determined on the basis of the Oliver and Pharr method [14]. The elastic modulus, E, was expressed as follows

$$\frac{1}{E_r} = \frac{1-\nu^2}{E} + \frac{1-\nu_i^2}{E_i} \tag{2}$$

where E_r and ν are the reduced modulus and Poisson's ratio, respectively, for the thin film under test, and E_i (1,140 GPa) and ν_i (0.07) are the corresponding parameters of the diamond indenter. A Vickers microhardness tester was used to further evaluate the indentation toughness, K, of coatings on Si substrates based on the following equation [15]:

$$K = \delta\left(\frac{P}{c^{3/2}}\right)\sqrt{\frac{E}{H}} \tag{2}$$

where P is the applied indentation load and δ is an indenter geometry constant, equal to 5 N and 0.016, respectively, for a Vickers diamond pyramid indenter. E, H and c are elastic modulus, hardness and radial crack length of the coating, respectively. The radial crack length was evaluated using an SEM.

A scratch test (Scratch Tester, J & L Tech. Co., Korea), up to a maximum load of 100 N, and the Daimler—Benz Rockwell-C (HRC-DB) adhesion test were adopted to explore the adhesion properties of thin films on TiC substrates. A pin-on-disc wear test method, in air, without lubrication, was used to investigate the wear resistance of coatings on Si substrates. A cemented tungsten carbide (WC–6 wt.% Co) ball, 5 mm in diameter was adopted as the stationary pin. A normal load of 5 N was applied. The sliding speed was 83.9 mm/s with a wear track diameter of 8 mm. The test temperature was 20 °C, and the relative humidity was kept at 60%. The wear time and wear length were 30 min and 150 m, respectively, for each test. The wear rate of each coating was determined based on the following equation [16]:

$$W_R = \frac{t\left(3t^2 + 4b^2\right)2\pi r}{6bF_nS} \tag{3}$$

where t is the depth of the wear track determined using a surface profilometer, b is the width of the wear track, r is the radius of the wear track, F_n is the normal load and S is the sliding distance.

Table 1
Deposition parameters for monolayer CrN, ZrN and CrN/ZrN multilayered coatings.

Sample designation	CrN	ZrN	B06	B08	B13	B15
Designed bilayer period (nm)	–	–	16			
Holder rotation speed (Hz)	7.5					
Cr target current (A)	70	0	105	91	70	70
Zr target current (A)	0	70	70	70	91	105
Base pressure (Pa)	1.0×10^{-2}					
Plasma etching	Ar plasma for 15 min at 1.2 Pa under substrate bias −750 V					
CrZr interlayer thickness (nm)	60					
Working pressure (Pa)	8.6×10^{-1}					
Substrate temperature (°C)	150					
Ar:N_2 ratio	1:7					
Total gas flows (sccm)	80					
Substrate bias (V)	−100					
Sputtering time (min)	24					

3. Results and discussion

3.1. Composition and phase characterization of CrN/ZrN multilayers

The chemical compositions of monolayer CrN, ZrN and CrN/ZrN multilayer coatings deposited with different Cr/Zr target current ratios are listed in Table 2. It is observed that the Cr/Zr atomic ratios changed from 1.0 to 2.5 as target current ratio changed from 0.6 to 1.5 as listed in Table 1. The glancing angle XRD patterns of monolayer CrN, ZrN and CrN/ZrN multilayer coatings deposited with different Cr/Zr atomic ratios are shown in Fig. 1. The precise lattice parameter, a_0, of each film, calculated based on the XRD results and Eq. (1), is listed in Table 2. The (111), (200), (220) and (311) reflections of the single layer CrN and ZrN coatings were observed, respectively. In addition, the XRD peaks of the Si substrate were also revealed due to a high X-ray incidence angle, 2°, used to penetrate the coating. For the CrN/ZrN multilayer coatings, some of the ZrN and CrN characteristic reflections can be observed for each coating. However, as compared with the monolayer coatings, different XRD reflection intensities were observed for multilayered coatings. The diffraction peak of CrN (200) vanishes whereas reflections along CrN (111) and ZrN (111) planes were formed in the multilayered thin films. A

Table 2
Characteristics of coatings: chemical composition, lattice parameter, adhesion strength, coating thickness and surface roughness.

Sample designation		CrN	ZrN	B06	B08	B13	B15
Cr/Zr target current ratio		–	–	1.5	1.3	0.7	0.6
ℓ_{CrN}/ℓ_{ZrN} thickness ratio		–	–	3.1	2.7	2.0	1.8
Chemical composition (at.%)	Cr	44.5	–	39.5	36.1	31.9	28.9
	Zr	–	60.0	15.8	17.1	24.6	28.6
	N	53.1	36.4	44.7	46.8	43.4	42.1
	O	2.4	3.6	0	0	0.1	0.4
	Cr/Zr ratio	–	–	2.5	2.1	1.3	1.0
Lattice parameter (nm)	CrN	0.417	–	0.420	0.421	0.426	0.425
	ZrN	–	0.459	0.445	0.447	0.455	0.453
Scratch critical load	L_{c2}(N)	>100	>100	>100	>100	>100	>100
HF value		1	3	1	1	1	1
Coating thickness (nm)		400	420	574	565	577	571
Surface roughness (nm)		1.1 ± 0.43	0.24 ± 0.02	2.76 ± 1.27	2.02 ± 1.70	2.95 ± 1.05	1.93 ± 1.18

similar result was also observed for CrN/ZrN multilayer coatings by Zhang et al. [7].

When the Cr/Zr atomic ratios decrease from 2.5 to 1, the positions and intensities of the CrN diffraction peaks shifted to higher diffraction angles and became weaker, respectively. On the other hand, the positions and intensities of the ZrN diffraction peaks shifted toward lower diffraction angles and became stronger, respectively. Based on the lattice parameter result of each multilayer coating, it is clear that the lattice constant of CrN increases with increasing Cr/Zr atomic ratio, whereas the decreasing tendency is found for the lattice constant of ZrN. For example, the lattice expansion of ZrN for specimen B06 is about 0.014 nm as compared with the lattice parameter of pure ZrN, 0.459 nm. Obviously, the change of Cr/Zr atomic ratios will affect the crystal structure of the multilayer thin films. Fig. 2 depicts the X-ray reflectivity patterns of CrN/ZrN multilayers with calculated Λ value. The Λ value was calculated based on a modified form of Bragg's law [17]:

$$\sin 2\theta = (m\lambda/2\Lambda)^2 + 2\delta, \quad (4)$$

where m is the order of the reflection, λ is the X-ray wavelength, Λ is the bilayer period thickness and δ is the real part of the average refractive index of X-rays within the film [17]. According to Fig. 2, the calculated Λ value is slightly smaller than the value we designed for, 16 nm, for each coating. A maximum deviation around 6.89% was found for the B08 coating. The multilayered thicknesses were confirmed through the XRR technique.

3.2. Microstructure characterization of CrN/ZrN multilayers

Based on the AFM analysis, a typical fine granular structure with macroparticles and pin holes was observed on the surface of each coating. It is suggested that the arc discharge on the target surface produced metallic macroparticles which were then splattered onto the coating surface during deposition [1]. The spalling of macroparticles thus produced the so-called pin holes on the thin film surface, which were several tens to hundreds nanometers in depth. Almost all of the pin holes are on the top surface layer of the coating. The average surface roughness, Ra, evaluated by AFM for each thin film is listed in Table 2. In general, the value of the bilayer period shows no direct influence on the surface roughness of the multilayer coating. Fig. 3 depicts the cross-sectional backscattered electron image (BEI) of the B13 coating. A dense and compact multilayer structure with columnar grains was observed. A CrZr interlayer can be seen between the coating and Si substrate. Very similar results can be found for other multilayer coatings. The thickness values of all coatings are listed in Table 2. Thickness values ranging from 565 to 577 nm were observed. However, for the case of the B06 coating with a Cr/Zr atomic ratio of 2.5, the multilayered nanostructure is difficult to recognize

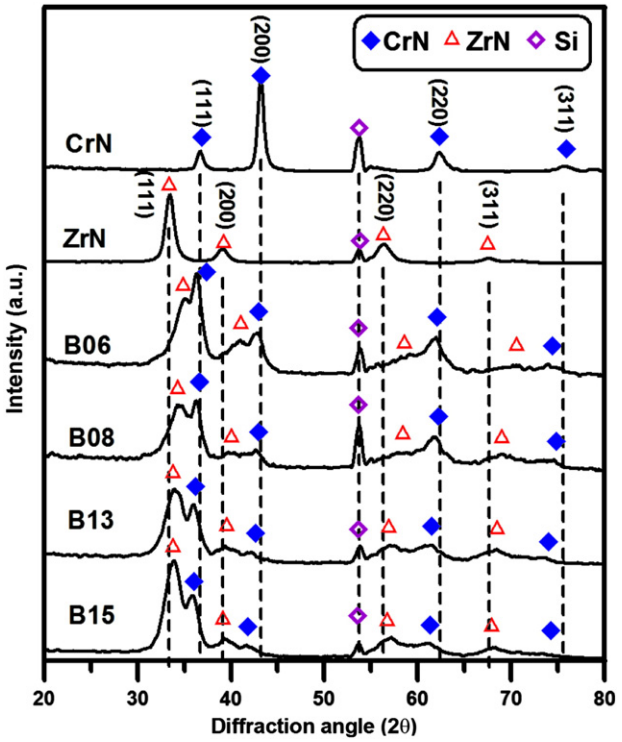

Fig. 1. Glancing angle X-ray diffraction patterns of the CrN, ZrN and CrN/ZrN multilayered coatings with various Cr/Zr atomic ratios on Si substrates.

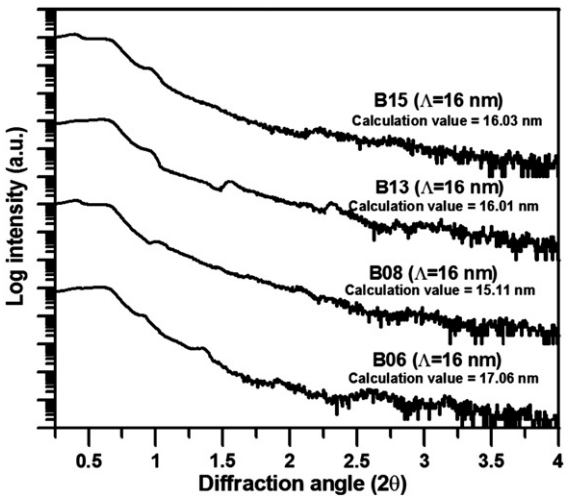

Fig. 2. X-ray reflectivity patterns of the CrN/ZrN multilayered thin films on Si substrates.

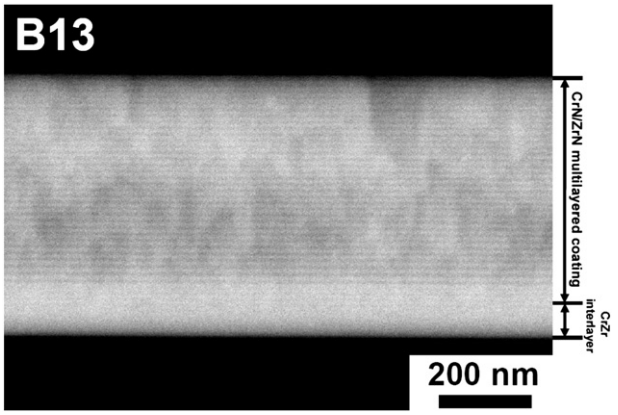

Fig. 3. The cross-sectional SEM morphology of the B13 multilayered coating on Si substrate.

due to the resolution limits of the FE-SEM. The TEM technique was further adopted to explore the detailed microstructure of multilayer coatings B08 and B15 with Cr/Zr atomic ratio = 2.1 and 1, respectively.

The cross-sectional TEM micrographs of B08 and B15 coatings at higher magnification are shown in Fig. 4(a) and (b), respectively. The clearly defined laminated and columnar structures can be observed. The alternating gray and dark color regions represent the CrN and ZrN layers (indicated by arrows), respectively. The average thickness values of the CrN and ZrN layers are 10.36 nm and 3.88 nm for B08 thin films, respectively. On the other hand, the average thickness values of the CrN and ZrN layers are 9.80 nm and 5.45 nm for B15 thin films, respectively. The layer thickness values of CrN and ZrN for each multilayer coating are determined and listed in Table 2. As compared with the Cr/Zr atomic ratios and the ℓ_{CrN}/ℓ_{ZrN} ratios in Table 2, a linear relationship between these two ratios is clearly found for the CrN/ZrN multilayer coatings indicating that through the proper adjustment of the Cr and Zr target currents, the corresponding Cr/Zr atomic ratios and ℓ_{CrN}/ℓ_{ZrN} ratios can be achieved. In the following sections, the ℓ_{CrN}/ℓ_{ZrN} ratios will be used to discuss the relevant properties of coatings.

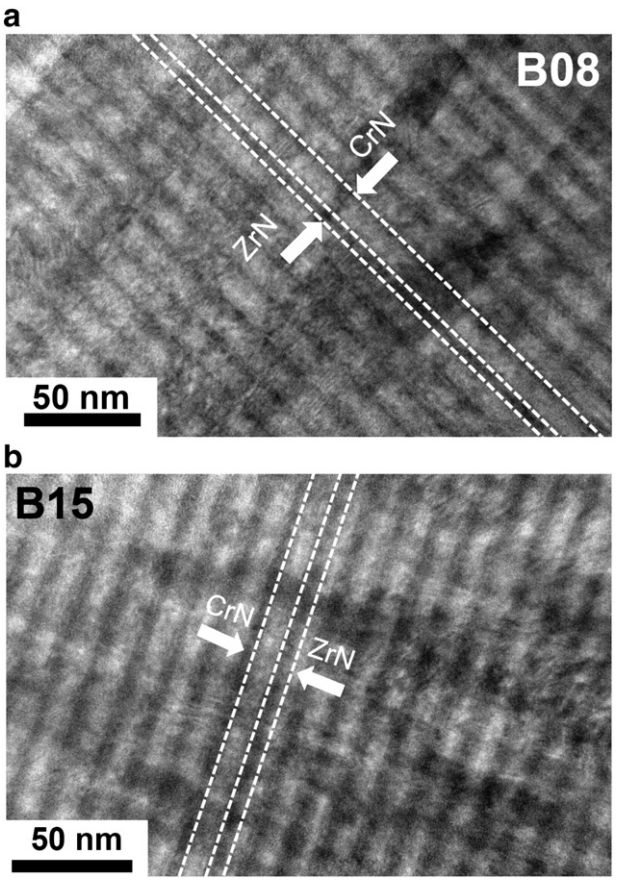

Fig. 4. Cross-sectional TEM micrographs of the (a) B08 and (b) B15 coatings on Si substrate at higher magnifications.

According to the cross-sectional SEM and TEM micrographs shown in Figs. 3, 4 and the XRR data revealed in Fig. 2, the nanolayered structures with sequentially alternating CrN and ZrN layers are confirmed. It is also concluded that the Λ value deviates from the design value less than 11%. Finally, the CrN/ZrN multilayered coatings do not belong to the superlattice type due to the large mismatch between CrN and ZrN lattices, about 10% in this work.

3.3. Mechanical and tribological properties of CrN/ZrN multilayered thin films

The hardness, elastic modulus and plastic deformation resistance values, H/E of the CrN/ZrN multilayered coatings as a function of ℓ_{CrN}/ℓ_{ZrN} ratios are shown in Fig. 5. The hardness, elastic modulus and plastic deformation resistance values of the monolayer CrN and ZrN coatings are also inserted. The average hardness and elastic modulus of monolayer CrN and ZrN are 20.3, 228 GPa and 21.9, 267 GPa, respectively. It is observed that the hardness is low, around 22–23 GPa when ℓ_{CrN}/ℓ_{ZrN} ratio is around 1.8–2.0 and reaches a maximum value, 28.8 GPa at $\ell_{CrN}/\ell_{ZrN} = 2.7$ and is followed by a decrease when $\ell_{CrN}/\ell_{ZrN} = 3.1$. Maximum hardness, elastic modulus, and plastic deformation resistance values reaching 28.8 GPa, 267 GPa, and 0.11, respectively, were observed for the B08 coating with $\ell_{CrN}/\ell_{ZrN} = 2.7$, whereas minimum hardness, elastic modulus and plastic deformation resistance values of 22.1 GPa, 253 GPa and 0.09 were found for the B15 coating with $\ell_{CrN}/\ell_{ZrN} = 1.8$. It should be pointed out that the hardness and elastic modulus of each CrN/ZrN multilayered coating are still higher than that of the single layer CrN or ZrN thin films. It can be concluded that the ℓ_{CrN}/ℓ_{ZrN} ratio or the Cr/Zr atomic ratio plays a critical role in the mechanical properties of CrN/ZrN multilayer coatings.

The indentation toughness, K, of the CrN/ZrN multilayered coatings versus the ℓ_{CrN}/ℓ_{ZrN} ratio is shown in Fig. 5. The toughness values of the monolayer CrN and ZrN coatings are around 2.06 MPa $\sqrt{m}$ and 1.83 MPa $\sqrt{m}$, respectively. In comparison, the values of toughness for

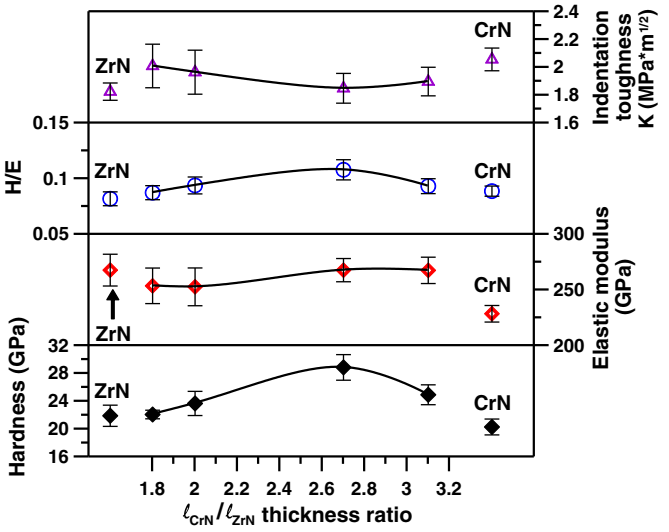

Fig. 5. The relationships between the hardness, elastic modulus, plastic deformation resistance, indentation toughness and ℓ_{CrN}/ℓ_{ZrN} thickness ratio for the CrN/ZrN multilayered coatings on Si substrates.

multilayered coatings are between those of the CrN and ZrN coatings ranging from 1.85 to 2.01 MPa $\sqrt{m}$. The maximum indentation toughness value, 2.01 MPa $\sqrt{m}$ can be found for the B15 coating at $\ell_{CrN}/\ell_{ZrN} = 1.8$, whereas the minimum toughness value, 1.85 MPa $\sqrt{m}$ can be found for the B08 coating at $\ell_{CrN}/\ell_{ZrN} = 2.7$ However, the actual mechanism for the dependence of ℓ_{CrN}/ℓ_{ZrN} ratio on the indentation toughness still needs further study. It is suggested that through a suitable control of the ℓ_{CrN}/ℓ_{ZrN} ratio or the Cr/Zr atomic ratio, a multilayered coating can act as a crack inhibitor while achieving the high hardness, adequate fracture resistance and high toughness values simultaneously [18,19].

As compared with the hardness values of CrN and ZrN monolayers, 20.3 and 21.9 GPa, respectively, strengthening from 22.1 to 28.9 GPa was observed for the CrN/ZrN multilayered coatings with $\Lambda = 16$ nm at $\ell_{CrN}/\ell_{ZrN} > 1.8$ in this work. Previous research work on the effect of individual layer thickness on the hardness enhancement effect of CrN based multilayered coating has been limited and has shown contradictory or conflicting results [12,20–22]. The dependence of hardness enhancement effect on individual layer thickness of TiAlN/CrSiN multilayered coating has been reported in a previous work [12]. It was observed that the hardness enhancement increased when the thickness of high modulus layer, TiAlN, increased and the thickness of low modulus layer, CrSiN decreased [12]. According to the research work by Chu and Barnett [20], varying the individual layer thicknesses had relatively little effect on the strength enhancement. On the other hand, a hardness decrease was reported by Nordin and Larsson [21] for the TiN/CrN multilayered coatings when the layer thickness of CrN was higher than that of TiN. Lewis et al. [22] reported that the maximum Knoop hardness of HK 3500 was obtained for the TiAlN/CrN multilayered coating when the thickness of the individual layers was equal. In this work, the shear modulus values of the CrN and ZrN are calculated to be 95 GPa and 111 GPa, respectively, using the Poisson's ratio of 0.2 for both CrN and ZrN and elastic modulus of 228 and 267 GPa for CrN and ZrN films. Therefore, according to Fig. 5, the hardness enhancement increases when the ℓ_{CrN}/ℓ_{ZrN} ratios increase from 1.8 to 2.7. This indicates that the hardness increases when the thickness of low modulus layer, CrN increases and the thickness of high modulus layer, ZrN, decreases, which is contradictory to the findings in previous work [12]. Consequently, the extent and causes of strengthening in CrN/ZrN multilayered coatings in this work still need further investigation.

According to the HRC-DB test [23], the adhesion level from HF1 to HF4 exhibits sufficient adhesion quality, whereas HF5 and HF6 represent insufficient adhesion. In this work, the HF values of all CrN/ZrN multilayered coatings were HF1. Obviously, all coatings exhibit excellent adhesion because no spallation occurred after 1470 N indentation loads. Spallation at this load has been reported in a previous work [11]. No spallation or chipping of coatings was found. Only very tiny radial cracks adjacent to the impact crater can be observed. Meanwhile, the critical load obtained from the scratch test can be used to estimate the adhesion of the coatings. The critical loads of all monolayer and multilayered coatings are higher than 100 N, indicating that excellent adhesion was achieved in this study. No cracking or delamination of coatings inside or adjacent to the scratch track was observed.

Fig. 6 illustrates the coefficient of friction (COF), measured by pin-on-disc wear test, versus the wear length of all thin films. A zigzag type COF curve is found for the ZrN coating, indicating that the ZrN coating was worn through after sliding wear of only 20 m. The average COF values and wear rates versus ℓ_{CrN}/ℓ_{ZrN} ratios are shown in Fig. 7. The COF values of monolayer CrN and ZrN were 0.48 and 0.53, respectively. A minimum COF around 0.41 was found for the B06 coating with $\ell_{CrN}/\ell_{ZrN} = 3.1$. A rather low COF value, 0.45, was also obtained for the B08 coating with $\ell_{CrN}/\ell_{ZrN} = 2.7$. The B06 films show significant lower wear rate, 3.62×10^{-7} mm^3 N^{-1} m^{-1}, as compared with other examined coatings, whereas the lowest wear

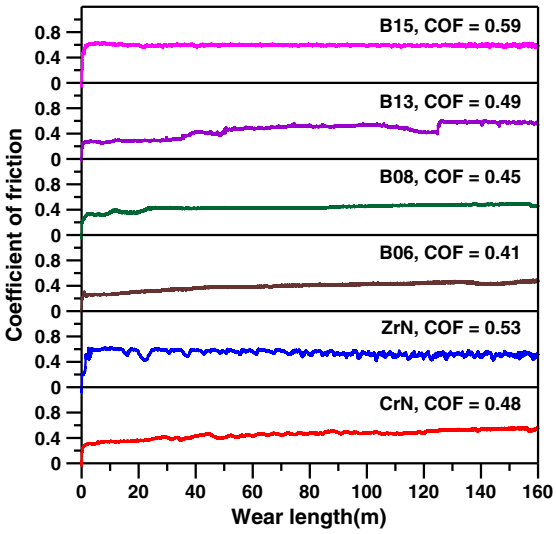

Fig. 6. The coefficient of friction of the CrN, ZrN and CrN/ZrN multilayered coatings on Si substrates against a WC–Co ball as a function of wear length.

rate, 3.45×10^{-7} mm^3 N^{-1} m^{-1}, was found for the CrN monolayer. However, the highest wear rate, 4.26×10^{-4} mm^3 N^{-1} m^{-1}, was obtained for B15 films. For multilayered coatings, it is obvious that the COF values and wear rates decrease with increasing ℓ_{CrN}/ℓ_{ZrN} ratios. It is suggested that the better COF values and lower wear rate of multilayered coatings with high ℓ_{CrN}/ℓ_{ZrN} ratios can be attributed to the thicker layer of CrN, which exhibits high indentation toughness and good wear resistance. On the other hand, the poor wear resistance of multilayer coatings with higher ZrN thickness, i.e., lower ℓ_{CrN}/ℓ_{ZrN} ratio, is caused by the brittle and poor wear resistance nature of the monolayer ZrN layer. In the wear study of the CrSiN/ZrN multilayered coatings, a better wear resistance for the coating with thicker CrSiN layer was also reported [6]. It is suggested that the hard and brittle ZrN coating cracked and became wear debris penetrating the multilayer coating and thus made the wear resistance worse during the wear test. The wear scar morphologies of the coating after the pin-on-disc tests were explored. In Fig. 8(a), a smooth wear track with a bit of cracking and delamination was observed on the wear track for B06 coating. On the other hand, the B15 coating was worn through after wear test as shown in Fig. 8(b), which was further confirmed by the chemical analysis of Si substrate using the energy dispersive spectrometer (EDS).

In the literature, the COF values and the wear rates for CAE fabricated CrN single layer and CrN based multilayered coating systems are quite different. For example, the COF and wear rate for CrN film were 0.54,

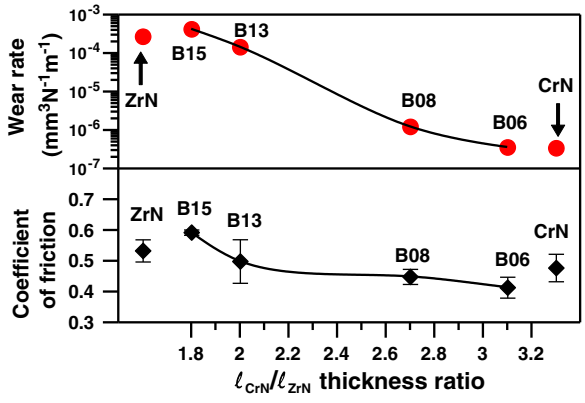

Fig. 7. The average COF values and wear rate versus l_{CrN}/l_{ZrN} thickness ratio of the CrN, ZrN and multilayered coatings on Si substrates.

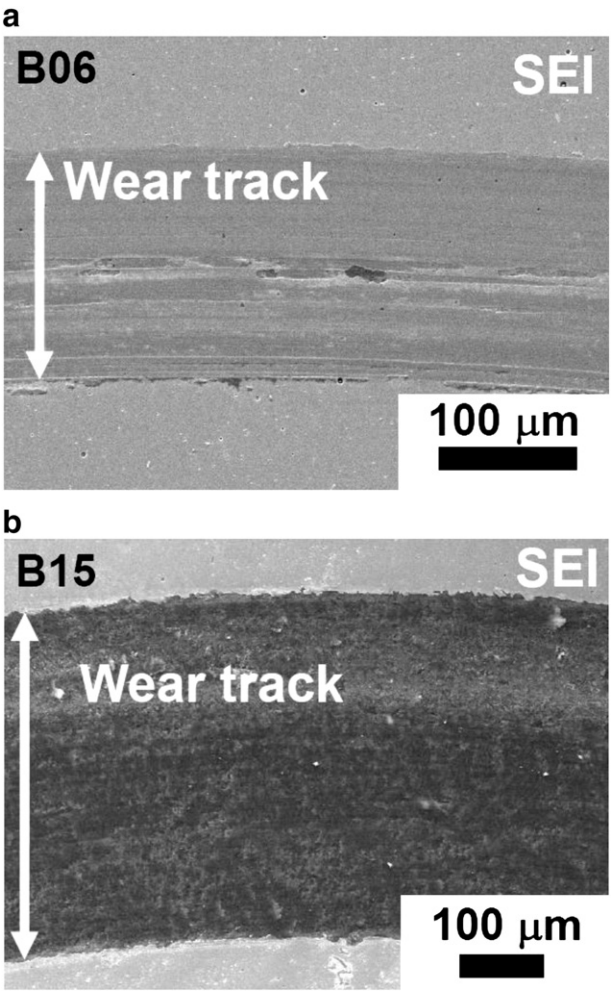

Fig. 8. The wear scar morphologies of the (a) B06 and (b) B15 coatings after the pin-on-disc test.

7×10^{-7} mm^3 N^{-1} m^{-1} [24] and 0.77, 8.93×10^{-7} mm^3 N^{-1} m^{-1} [25], respectively. On the other hand, much lower friction coefficient (0.39) and wear rate (1.3×10^{-7} mm^3 N^{-1} m^{-1}) for CrN coatings deposited using a large area filtered cathodic arc evaporation technique were reported [24]. Meanwhile, the COF values and wear rates for the CAE deposited TiAlN/CrN and CrN/NbN multilayer coatings were 0.16, 0.61 and 2.38×10^{-7}, 2.10×10^{-6} mm^3 N^{-1} m^{-1}, respectively [26]. It is obvious that the COF values and wear rates for CrN monolayer and B06 CrN/ZrN multilayer thin films in this work are comparable to other studies [24–26].

It can be concluded that the hardness and wear resistance of the CrN/ZrN multilayer coating were enhanced by increasing the Cr/Zr atomic ratio or ℓ_{CrN}/ℓ_{ZrN} thickness ratio in this work. Although the ZrN coating is characterized by its good hardness, a detrimental effect of ZrN layer thickness to the tribological property of the CrN/ZrN multilayer coating has been discovered, which is attributed to the low indentation toughness, brittle nature [11] and rather high wear rate [4] of the CrN/ZrN coating.

4. Conclusions

Four CrN/ZrN multilayered thin films with fixed $\Lambda = 16$ nm and different Cr/Zr atomic ratios or ℓ_{CrN}/ℓ_{ZrN} ratios ranging from 1 to 2.5, or 1.8 to 3.1, respectively, were prepared by a cathodic arc evaporation process in this study. Typical CrN and ZrN crystal structures were observed for the multilayered coating. When the Cr/Zr atomic ratio decreased, the positions of the CrN diffraction peaks shifted to higher diffraction angles and the intensity also decreased. For the multilayer coatings, the lattice constant of CrN increased with increasing Cr/Zr atomic ratios, whereas a decreasing tendency was found for the lattice constant of ZrN. Excellent adhesion property was observed for each coating. It was found that the wear resistance of the coating was enhanced by increasing the Cr/Zr atomic ratio or ℓ_{CrN}/ℓ_{ZrN} ratio. A combination of excellent mechanical and adhesion properties, high plastic deformation resistance and good tribological performance was achieved for the CrN/ZrN multilayered coating with the Cr/Zr atomic ratio of 2.1 and $\ell_{CrN}/\ell_{ZrN} = 2.7$ in this work.

Acknowledgement

The authors gratefully acknowedge the financial support of the National Science Council, Taiwan through contract no. NSC100-2622-E-131-001-CC2.

References

[1] R.L. Boxman, S. Goldsmith, Surf. Coat. Technol. 52 (1992) 39.
[2] S. Ulrich, C. Ziebert, M. Stuber, E. Nold, H. Holleck, M. Goken, E. Schweitzer, P. Schloßmacher, Surf. Coat.Technol. 188 (2004) 331.
[3] X.M. Xu, J. Wang, J. An, Y. Zhao, Q.Y. Zhang, Surf. Coat.Technol. 201 (2007) 5582.
[4] J.J. Zhang, M.X. Wang, J. Yang, Q.X. Liu, D.J. Li, Surf. Coat.Technol. 201 (2007) 5186.
[5] D.J. Li, F. Lin, M.X. Wang, J.J. Zhang, Q.X. Liu, Thin Solid Films 506 (2006) 202.
[6] Z.G. Zhang, O. Rapaud, N. Allain, D. Mercs, M. Baraket, C. Dong, C. Coddet, Adv. Eng. Mater. 11 (2009) 667.
[7] Z.G. Zhang, O. Rapaud, N. Allain, D. Mercs, M. Baraket, C. Dong, C. Coddet, Appl. Surf. Sci. 255 (2009) 4020.
[8] J. Barranco, F. Barranco, A. Lozano, A.M. Lopez, V. Roda, J. Martin, M. Maza, G.G. Fuentes, E. Almandoz, Int. J. Hydrogen Energy 35 (2010) 11489.
[9] N.A. de Sánchez, H.E. Jaramillo, Z. Vivas, W. Aperador, C. Amaya, J.C. Caicedo, Adv. Mater. Res. 38 (2008) 63.
[10] R. Bayón, R. Nevshupa, C. Zubizarreta, U. Ruiz de Gopegui, J. Barriga, A. Igatua, Anal. Bioanal. Chem. 396 (2010) 2855.
[11] S.H. Huang, S.F. Chen, Y.C. Kuo, C.J. Wang, J.W. Lee, Y.C. Chan, H.W. Chen, J.G. Duh, T.E. Hsieh, Surf. Coat.Technol. 206 (2011) 1744.
[12] M.K. Wu, J.W. Lee, Y.C. Chan, H.W. Chen, J.G. Duh, Surf. Coat.Technol. 206 (2011) 1886.
[13] B.D. Gullity, S.R. Stock, Prentice Hall, NJ, 2001, p. 367.
[14] M.C. Oliver, G.M. Pharr, J. Mater. Res. 7 (4) (1992) 1564.
[15] B.R. Lawn, A.G. Evans, D.B. Marshall, J. Am. Ceram. Soc. 63 (1980) 574.
[16] S. Ma, J. Procházka, P. Karvánková, Q. Ma, X. Niu, X. Wang, D. Ma, K. Xu, S. Veprek, Surf. Coat.Technol. 194 (2005) 143.
[17] P.C. Yashar, W.D. Sproul, Vacuum 55 (1999) 179.
[18] P. Panjan, M. Čekada, B. Navinšek, Surf. Coat.Technol. 174 (2003) 55.
[19] M. Stueber, H. Holleck, H. Leiste, K. Seemann, S. Ulrich, C. Ziebert, J. Alloys Compd. 483 (2009) 321.
[20] X. Chu, S.A. Barnett, J. Appl. Phys. 77 (1995) 4403.
[21] M. Nordin, M. Larsson, Surf. Coat.Technol. 116–119 (1999) 108.
[22] D.B. Lewis, I. Wadsworth, W.-D. Münz, R. Kuzel Jr., V. Valvoda, Surf. Coat.Technol. 116–119 (1999) 284.
[23] H. Jehn, G. Reiners, N. Siegel (Eds.), DIN Fachbericht 39, Characterisierung DunnerSchichten, Beuth Verlag, Berlin, 1993, p. 213.
[24] B. Warcholiński, A. Gilewicz, Z. Kukliński, P. Myśliński, Vacuum 83 (2009) 715.
[25] Y.H. Cheng, T. Browne, B. Heckerman, Wear 271 (2011) 775.
[26] W.-D. Münz, L.A. Donohue, P.Eh. Hovsepian, Surf. Coat.Technol. 125 (2000) 269.